

LETTER • OPEN ACCESS

Periodic decadal swings in dry/wet conditions over Central Asia

To cite this article: Yusen Liu *et al* 2022 *Environ. Res. Lett.* **17** 054050

View the [article online](#) for updates and enhancements.

You may also like



- [High-stability inorganic perovskite quantum dot–cellulose nanocrystal hybrid films](#)
Chih-Hao Chiang, Ting-You Li, Han-Song Wu et al.
- [CsPbCl₃ perovskite quantum dots/TiO₂ inverse opal photonic crystals for efficient photoelectrochemical detection of alpha fetoprotein](#)
Jiaqiong Qin, Shaobo Cui, Xingqiang Yang et al.
- [Highly efficient silica-coated Eu³⁺ and Mn²⁺ doped CsPbCl₃ perovskite quantum dots for application in light-emitting diodes](#)
Yinhua Wang, Yongsheng Zhu, Gang Yang et al.

ENVIRONMENTAL RESEARCH
LETTERS

LETTER

Periodic decadal swings in dry/wet conditions over Central Asia

OPEN ACCESS

Yusen Liu¹, Cheng Sun^{1,*} , Zengchao Hao²  and Bian He³RECEIVED
23 January 2022REVISED
18 April 2022ACCEPTED FOR PUBLICATION
3 May 2022PUBLISHED
16 May 2022

Original content from
this work may be used
under the terms of the
[Creative Commons
Attribution 4.0 licence](#).

Any further distribution
of this work must
maintain attribution to
the author(s) and the title
of the work, journal
citation and DOI.

¹ College of Global Change and Earth System Science (GCESS), Beijing Normal University, Beijing, People's Republic of China² Green Development Institute, College of Water Sciences, Beijing Normal University, Beijing, People's Republic of China³ Institute of Atmospheric Physics, Chinese Academy of Sciences, Beijing, People's Republic of China

* Author to whom any correspondence should be addressed.

E-mail: scheng@bnu.edu.cn**Keywords:** decadal oscillation, Pacific quasi-decadal oscillation, Central Asian dry/wet conditions, periodic climate variabilitySupplementary material for this article is available [online](#)**Abstract**

Periodic variability in the hydro-climatic system has important implications not only for climate prediction but also for planning and managing water resources. Here we identify periodic decadal variability of dry/wet conditions in Central Asia (CA) since the mid-20th century, which are tied to the Pacific quasi-decadal oscillation (PQDO) with a period of 8–16 years ($r = 0.87$). The periodically varying forcing in the Pacific modulates zonal winds and moisture transport and profoundly affects the precipitation on the decadal time scale. The PQDO-related equatorial central Pacific warming significantly heats the overlying troposphere, increasing the meridional temperature/geopotential gradients in the subtropics. As a result, the strengthened westerly jet in CA transports more water vapor from the North Atlantic and increases local precipitation. The plateau to the east further amplifies the increased precipitation in eastern CA through orographic influence on the convection and large-scale circulation. The atmospheric model forced by the PQDO signal reproduces an overall consistent mechanism with the observation, indicating a robust synchronization of the Central Asian hydro-climatic system to the PQDO. The newly discovered oscillatory feature in this study may advance the predictability of Central Asian precipitation on the decadal time scale, which promotes the mitigation and prevention of natural disasters like droughts and wildfires.

1. Introduction

The climate system has complex time-varying features, such as linear trend, periodic variability, and irregular fluctuation. The former two provide a vast majority of climate predictability, while the latter is stochastic noise from the nonlinear system [1]. Aside from the human-induced long-term trend, periodic variabilities are vital to predictions. Many previous studies have illustrated the oscillatory features in the climate system. The quasi-biennial oscillation [2, 3] is a dominating mode in the equatorial stratosphere and has a period of approximately 28 months, with alternating zonal winds propagating downward. On the interannual time scale, El Niño Southern Oscillation (ENSO) exhibits 2–7 years periodicity [4, 5], significantly affecting the global climate. On the inter-decadal to multidecadal time scales, the sea surface

temperature (SST) in the North Atlantic shows significant variations between the warm and cold phases that persist for 30–40 years, referred to as the Atlantic Multidecadal Oscillation (AMO) [6]. Due to large heat capacity, the oscillations found in the oceans are often sources of climate variability [7], causing synchronized oscillations in local and remote regions via teleconnection [8, 9]. As the periodically driven oscillations are often highly predictable [1], the predominant oscillatory features in the oceans may have great implications for more precise predictions of regional climate.

In the tropical Pacific, the interannual and inter-decadal oscillations, such as ENSO and Interdecadal Pacific Oscillation (IPO), have long been recognized, whereas less attention has been paid on the quasi-decadal scale. Previous studies detected a quasi-decadal signal in the equatorial central

Pacific (ECP), known as the Pacific quasi-decadal oscillation (PQDO) [10, 11]. The PQDO is identified as SST warming/cooling in the ECP region, with a significant period of 9–13 years since 1951 [10, 12]. The SST signal is originated from the subtropical North Pacific and amplified/sustained by meridional advection and deepening in the thermocline, while zonal advection is mainly responsible for its decay [12]. The 11 years cycle of the PQDO has been hypothesized by both external forcings related to the solar radiative cycle [13, 14] and internal variability associated with the nonlinear component of ENSO [15]. It is suggested that the PQDO could be distinguished from ENSO or the IPO since their periodicities and underlying dynamics are significantly different [12].

As a distinct mode of variability, the PQDO has profound impacts on remote regional climate via atmospheric teleconnection. For instance, Wang *et al* (2014) [16] have linked the quasi-decadal variation of North American rainfall to the phase-transition of PQDO. A wave train related to the PQDO propagates from Southeast Asia to North America and further changes the local hydrologic cycle, resulting in synchronized oscillations in the intermountain precipitation [17] and the Salt Lake water level [18]. The PQDO also leads the monsoonal precipitation in Nepal (southern Himalayan foothills) via enhanced moisture fluxes related to the PQDO-excited wave train [19]. Moreover, the PQDO influences the precipitation in Taiwan by the westward extension of the North Pacific subtropical anticyclone [20]. Above all, the quasi-decadal variations in many areas are synchronized or lagged to the PQDO. It could significantly improve the predicting skill regarding the PQDO as a precursor of regional climate.

Central Asia (CA), as one of the largest drylands in the Northern Hemisphere [21], is characterized by complex geographic landscapes, shortage of water resources, agriculture-led economies, and growing populations [22]. In the background of global warming, Central Asian surface air temperature has warmed at $0.36 \text{ K decade}^{-1}$, which is two times faster than the global mean [23], while the regional precipitation has decreased slightly [24]. Consequently, the drying climate and increasing water demands lead to more severe and frequent droughts [25], which significantly threaten the sustainable development of the Central Asian economy and society [26]. However, the current numerical prediction of Central Asian weather and climate is far from skillful. Therefore, it is urgent to improve the predictability of regional droughts in CA.

The drought condition in CA is modulated by both water supply and evaporative demand associated with local precipitation and air temperature, respectively, which exhibit significant interannual and interdecadal variabilities [27]. Previous studies have demonstrated that the air temperature in CA is modulated by the North Atlantic Oscillation (NAO),

AMO, and East Atlantic/West Russia pattern, while the precipitation shows close associations with ENSO [28] and the Scandinavia pattern [29, 30]. The CA precipitation exhibits oscillatory features, with periods of 3–6 and 28 years [31]. The interannual cycle is explained by ENSO, while the interdecadal oscillation may be more related to the NAO and Pacific decadal oscillation [27]. The variations in temperature and precipitation are embedded in the drought condition of CA, which also exhibits strong variabilities on multiple time scales. As many studies have focused on the CA aridity on interannual and multidecadal time scales [32], the decadal variability of dry/wet conditions is lesser-known. Previous studies have revealed a 16–64 months oscillation in Central Asian drought, which is closely related to ENSO [33, 34], indicating a close connection between CA and the tropical Pacific on the interannual time scale. However, does such a teleconnection exist on the decadal time scale remains unclear. As mentioned above, the oscillatory characteristic is an important source of predictability. Thus, investigating the periodicity in Central Asian dry/wet conditions and linking it to remote climate modes on the decadal time scale would greatly improve the prediction skills and contribute to disaster prevention and mitigation.

2. Method

2.1. Data

In this study, the monthly land surface data, including precipitation, soil moisture, surface temperature, and Palmer drought severity index (PDSI) for global terrestrial surfaces, are derived from the TerraClimate [35], which is a global dataset of meteorological and water balance variables (available at www.climatologylab.org/terraclimate.html). The TerraClimate dataset is based on station and reanalysis data and is available from 1958 to the present. The dataset has a rather high resolution at 4 km, which is then conformed to T63 grids ($1.88^\circ \times 1.88^\circ$) to match the resolution of atmospheric data. To verify the periodic decadal variability in Central Asian dry/wet conditions, we also examine other products. We use the self-calibrating PDSI (scPDSI) from the Climatic Research Unit (CRU) (<https://crudata.uea.ac.uk/cru/data/drought/>) at 0.5° spatial resolution for 1901–2018 [36]. The scPDSI over CA in CRU data shows a similar quasi-decadal periodicity with the TerraClimate (not shown here). The ERSSTv5 dataset is also employed [37], which has a resolution of 2° . The atmospheric reanalysis data, including geopotential height, water vapor, winds, and vertical motion, are from the JRA55 reanalysis [38], with a resolution of 1.25° . All data are analyzed for the period 1958–2018. Additionally, the ensemble mean of the Atmospheric Model Intercomparison Project (AMIP) simulation out of 24 CMIP6 models (supplementary

table 1 available online at stacks.iop.org/ERL/17/054050/mmedia) with 38 ensemble members is analyzed for the period 1979–2014. Most of the AMIP models (18 out of 24) have a horizontal resolution of less than 2° . AMIP is a standard experimental protocol for global atmospheric general circulation models (AGCMs) driven by the prescribed observed SST [39]. The simulated precipitation is used to examine the relationship between the PQDO and the Central Asian precipitation in comparison with the observation.

2.2. Computation of PDSI

The PDSI is a commonly used indicator to quantify the drought condition and has been employed in many previous studies [40, 41]. The PDSI is based on the water balance equation by taking both water supply and demand into consideration (e.g. incorporating precipitation and potential evapotranspiration (PET)). The calculation of PET is based on the Penman–Monteith equation [42]. Note that the PDSI has scale-fixed characteristics, with a preferable time scale of 9–12 months [43], which meets the requirements in the present study focusing on the annual dry/wet conditions. The time series is calculated by the area-weighted average of PDSI in CA (35°N – 45°N , 50°E – 75°E).

2.3. Statistical method

We apply a local wavelet spectrum method with a Morlet wavelet base [44] to analyze the oscillatory feature of one time series and gain its significant period. The decadal component of a series is computed by an 8–16 years band-pass filter. The statistical significance of the correlation coefficient is evaluated by a two-tail Student's t test. The effective number of degrees of freedom (N^{eff}) in the original series is estimated by:

$$\frac{1}{N^{\text{eff}}} \approx \frac{1}{N} + \frac{2}{N} \sum_{j=1}^N \frac{N-j}{N} \rho_{XX}(j) \rho_{YY}(j) \quad (1)$$

where N denotes the sample size and $\rho_{XX}(j)$ stands for the autocorrelation of sampled time series X and $\rho_{YY}(j)$ is for Y , while j is the time lag.

2.4. Central Pacific SST-forced-AGCM experiment (CP_EXP)

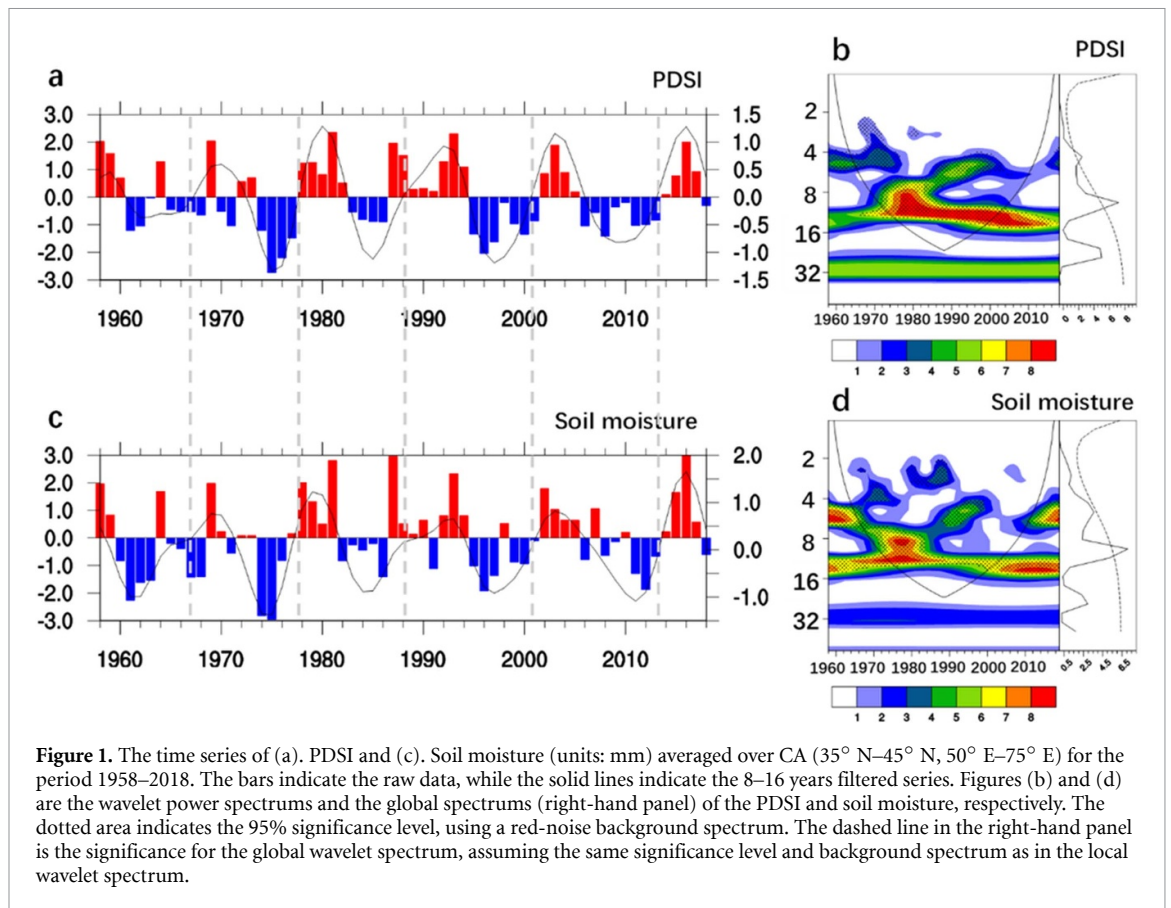
In this study, a CP_EXP is conducted to investigate the atmospheric response to the central Pacific SST and the associated precipitation changes in CA. This experiment employs the International Centre for Theoretical Physics AGCM version 41 (ICTPAGCM V41) [45], which has a horizontal resolution of T30 ($3.75^\circ \times 3.75^\circ$) with eight vertical levels. In the CP_EXP, the AGCM is forced by the observed monthly-varying SST over the central Pacific region (10°S – 10°N , 165°E – 165°W), and the climatological monthly SSTs are prescribed elsewhere. This experiment aims to directly assess the impact of SST

forcing on the atmospheric circulation and isolate the effects from the central Pacific and the PQDO signal. The CP_EXP simulations starts in 1940 and run through 2018. The first 19 years are for the model to spin up. An ensemble of five members is generated by restarting the model using small initial perturbations. All the members are transient runs. The results of the ensemble members are averaged and analyzed for the period 1958–2018. Therefore, the simulated atmospheric circulation changes associated with the PQDO signal can be considered as the direct response to the PQDO-related SST forcing. In order to inspect the effects of Asian topography on the responses of precipitation over CA, we perform an additional experiment similar to the CP_EXP, but with the East Asian topography removed (referred to as CP_EXP_NT) in the model simulation.

3. Results

3.1. Quasi-periodic variability in Central Asia (CA) dry/wet conditions

The PDSI quantifies the regional dry/wet conditions by considering the difference between water supply (precipitation) and demand PET and is a commonly used indicator for yearly meteorological droughts. As shown in figure 1(a), the PDSI (bar) in CA exhibits its notable interannual variability, varying within ± 3 , whereas the long-term trend is not significant. The positive (negative) PDSI indicates a wetter (drier)-than-normal condition. Visually, the wet/dry conditions alternatively persist for 4–5 years, which implies periodicity in the Central Asian dry/wet conditions. To verify this inference, we apply the Morlet wavelet analysis to the Central Asian PDSI for the period 1958–2018. In figure 1(b), the wavelet spectrum shows considerable energy at an 8–16 years frequency band during the whole analyzed period, indicating a quasi-periodic feature in the Central Asian dry/wet conditions. The corresponding power spectrum peaks at 8–16 years, indicating that the periodicity is most prominent on the decadal time scale. In order to highlight the decadal component, the series of PDSI is processed by 8–16 years band-pass filtering (figure 1(a), line), which shows a prominent quasi-periodic fluctuation, with wet/dry conditions alternatively occurring on the order of 4–8 years, consistent with the wavelet analysis. Note that the quasi-decadal periodicity of PDSI can be captured by 5 years low-pass filtering as well, which explains at least 50% of the decadal variance of the PDSI. It is not surprising because the prominent spectrum of PDSI is concentrated within the frequency band of 8–16 years, while the variance on the inter-decadal time scale is relatively minor. In addition to the PDSI, soil moisture is also an essential aspect of regional dry/wet conditions, which is vital to agricultural production. In figure 1(c), the interannual variability of soil moisture is generally consistent with

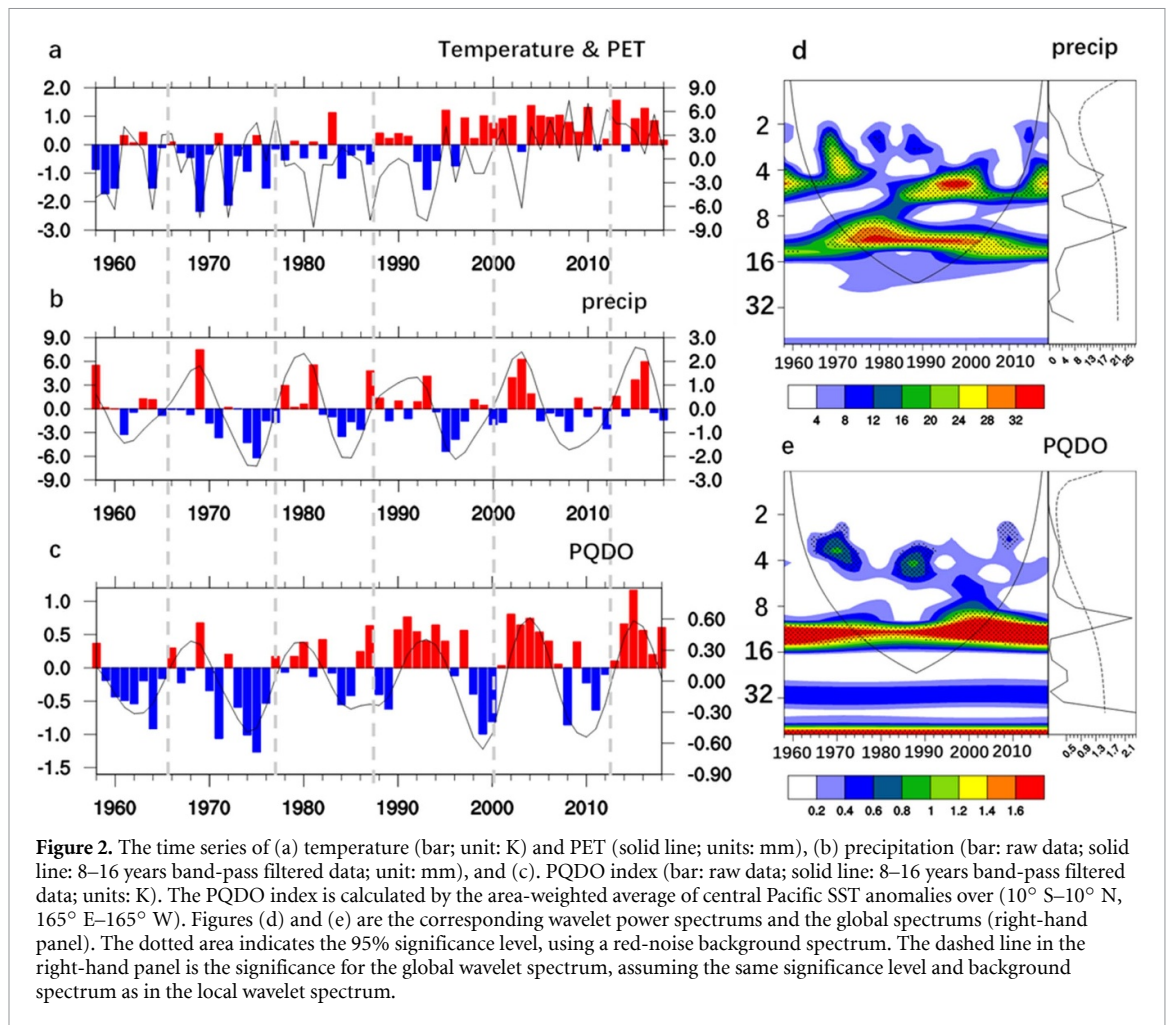


that of the PDSI ($r = 0.88$). Through the wavelet analysis (figure 1(d)), the quasi-periodic component of the soil moisture variability in CA is highlighted on the decadal time scale, with a peak power spectrum at 8–16 years. The band-pass filtered series of soil moisture exhibits an identical oscillatory feature. This has been consistently demonstrated by the results using cross wavelet transform (CWT) [46] methods, which suggests that the interannual variabilities of PDSI and the soil moisture are strongly correlated, together with similar wavelet power spectrums peaking at 8–16 years (supplementary figure 1(a)). We may conclude that the periodic decadal swings in the Central Asian hydro-climatic system are robust and independent of indicators that quantify the regional dry/wet conditions.

Based on the PDSI and soil moisture, we have found significant decadal periodicity in the Central Asian dry/wet conditions, but what drives the fluctuation is still unknown. For the PDSI, two factors are taken into consideration, one is precipitation, and the other is PET related to surface air temperature. Here, we inspect the time series of temperature, PET, and precipitation to find out which one dominates the quasi-periodic component of the PDSI in CA. In figure 2(a), the time series of surface air temperature (bar) in CA shows a significant long-term warming trend superimposed on the interannual variability. However, no significant periodicity on the decadal time scale can be found. It is suggested that the

Central Asian air temperature is modulated by the AMO, which exhibits a period of 50–70 years [47], with a phase shift in the 1990s, consistent with that in temperature. Thus, the long-term warming may be a passage of the multidecadal oscillation related to the AMO [29]. Meanwhile, anthropogenic forcing may also play a role [48]. As the temperature is an essential parameter in the computation of PET, the variations between them are overall agreed. It must be noted that both the surface air temperature and PET are consistently dominated by an increasing trend, whereas their decadal component of variabilities or their periodicities are obscure within the analyzed period. Thus, we may conclude that the variations in either temperature or the associated water demand contribute little to the observed decadal oscillation in PDSI over CA.

Other than the surface air temperature, precipitation is another major factor influencing the PDSI. Unlike surface air temperature, the oscillatory feature in precipitation is more pronounced, while the long-term trend is insignificant. The time series of CA precipitation is shown in figure 2(b). By applying the band-pass filtering (8–16 years), the decadal component of the precipitation variations is isolated. It fluctuates quasi-periodically within 8–16 years, which is consistent with the band-pass filtered series of the PDSI ($r = 0.91$), indicating a synchronized decadal variability. In figure 2(d), the energy in the wavelet analysis is concentrated in the frequency band of 8–16 years, which is also similar to the PDSI. In

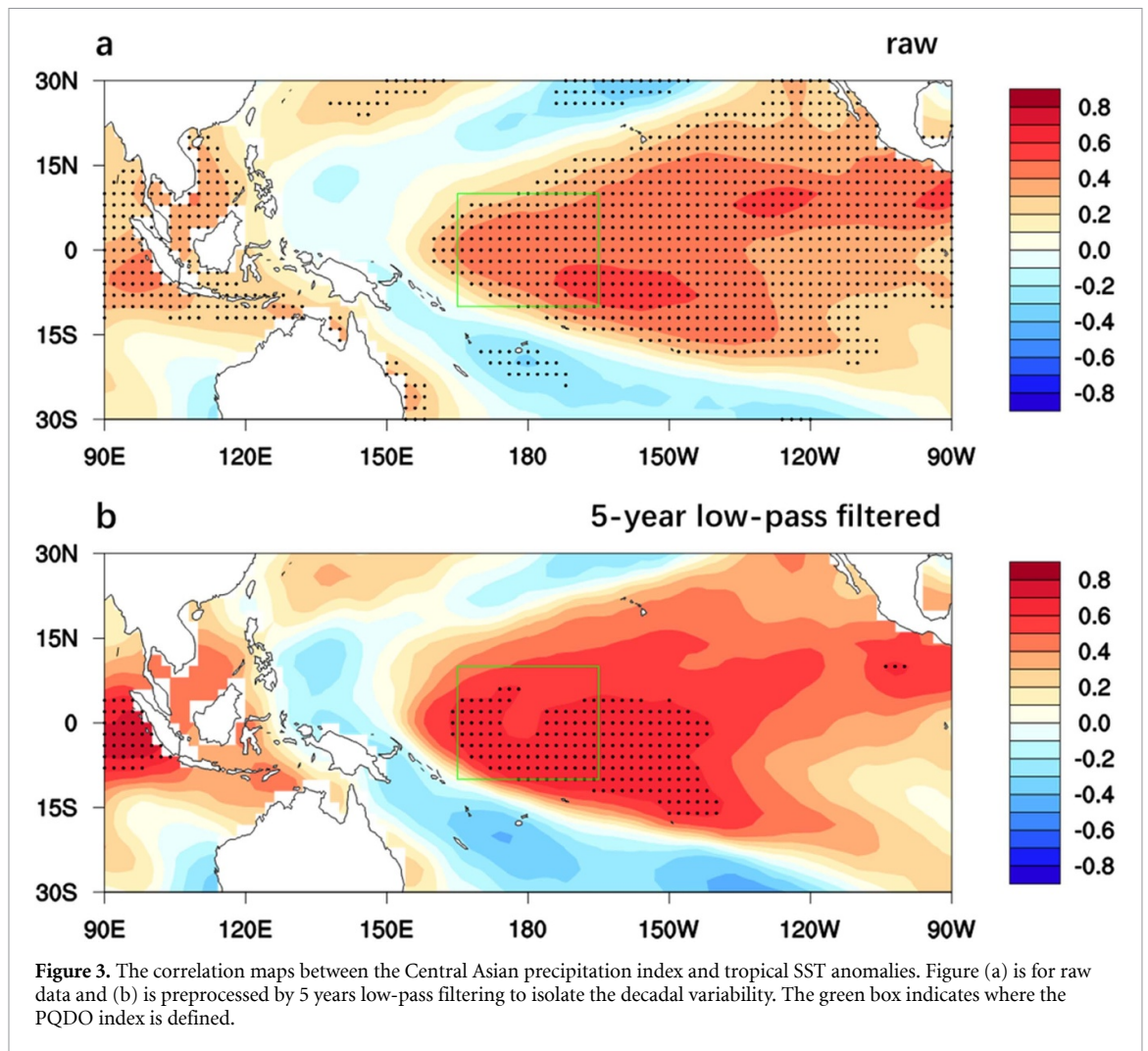


addition, the power spectrum also suggests that a period of 8–16 years prevails over the other cycles, further identifying periodic decadal swings in precipitation over CA. It must be noted that the power spectrum of precipitation also indicates a period of 4–5 years, which has been attributed to the ENSO variability in previous studies [31]. However, less attention has been paid to its decadal component of variability. Based on the above analysis, we can conclude that the decadal oscillation in Central Asian dry/wet conditions is mainly driven by the periodic variability in precipitation, while little contribution originated from the temperature/PET variabilities, which are dominated by a consistently increasing trend.

3.2. Linking the quasi-decadal oscillation to Central Pacific SST

As suggested above, precipitation anomaly is a direct driver of the decadal oscillation in the Central Asian dry/wet conditions. Thus, figuring out what modulates the precipitation on the decadal time scale may reveal the underlying mechanism of how the decadal periodicity is formed. As suggested in previous studies [8, 9], oscillations in the oceans can modulate the weather pattern and climate through teleconnections,

resulting in synchronized or lagged oscillatory features over the inland area. In order to seek potential drivers of the CA precipitation, we inspect the correlation map of the CA precipitation with tropical SST anomalies (figure 3(a)), and we also employ the 5 years low-pass filtered data to isolate the decadal component of variabilities. Interestingly, the Pacific Ocean basin exhibits the most significant coherence with the precipitation index on the interannual time scale. The Central Asian precipitation is positively correlated with the tropical central-eastern Pacific SST, while significant cooling can be found in the subtropical central Pacific and western Pacific. It is consistent with previous studies [31], which demonstrate that the interannual variability of Central Asian precipitation is largely modulated by ENSO. In addition, the ECP exhibits the most prominent warming, with a correlation coefficient larger than 0.5, further indicating a tight connection between central Pacific SST and Central Asian precipitation. In figure 3(b), the SST warming signal in the ECP is even more prominent via 5 years low-pass filtering, with the correlation coefficient exceeding 0.6. The SST warming extends from the ECP to the subtropical eastern Pacific in both hemispheres, while the eastern tropical Pacific warming is less significant. In the subtropical central



Pacific and tropical western Pacific, the SSTs show an arch-shaped cooling. Note that the correlation pattern based on the 8–16 years band-pass filtered data (not shown here) is similar to figure 3(b). It must be noted that the low-pass filtered correlation pattern is very similar to the PQDO, as is shown in the previous study [12], implying a potential linkage between the PQDO and the Central Asian precipitation on the decadal time scale.

Since the spatial coherence between the central Pacific SST and Central Asian precipitation has been identified on the decadal time scale, the temporal consistency should be examined. Here, we define the PQDO index by the area-weighted average of SST anomalies in the ECP (10° S–10° N, 165° E–165° W), consistent with the previous study [12]. As shown in figure 2(c), the decadal component of the PQDO (8–16 years band-pass filtered series) exhibits prominent quasi-periodic fluctuations, which is consistent with the Central Asian precipitation ($r = 0.78$) as well as the PDSI ($r = 0.87$). The spatial correlation between the PQDO index and the PDSI is also inspected (not shown here), which shows a significant positive correlation in CA, consistent with the time series analysis. However, the coherences between

PQDO and CA surface air temperature and PET are not valid. To verify the periodicity in PQDO, we apply the wavelet analysis on the PQDO index (figure 2(e)), which exhibits significant oscillatory features at a period of 8–16 years, with a spectrum peak at 11 years. The CWT pattern between the PQDO and the Central Asian precipitation (supplementary figure 1(c)) exhibits a strong coherence over the period of 8–16 years. The vectors pointing right at the frequency band 8–16 years are also prominent, indicating that the two series are quite in-phase. For instance, the phase shifts of PQDO in 1966, 1977, 2001, and 2013 generally correspond with those in the Central Asian precipitation. Despite that slight disagreement of phase shifts from 1977 to 2000, more precipitation in CA mostly corresponds to a warmer SST in the ECP. The periodic variability of the PQDO agrees with not only the Central Asian precipitation but also the PDSI. The CWT pattern between the PQDO and the Central Asian PDSI is also inspected (supplementary figure 1(b)). It is suggested that the frequency band of 8–16 years is most correlated between them, and the correlation coefficients are well above 0.8 throughout the whole analyzed period, indicating that the decadal periodicities are

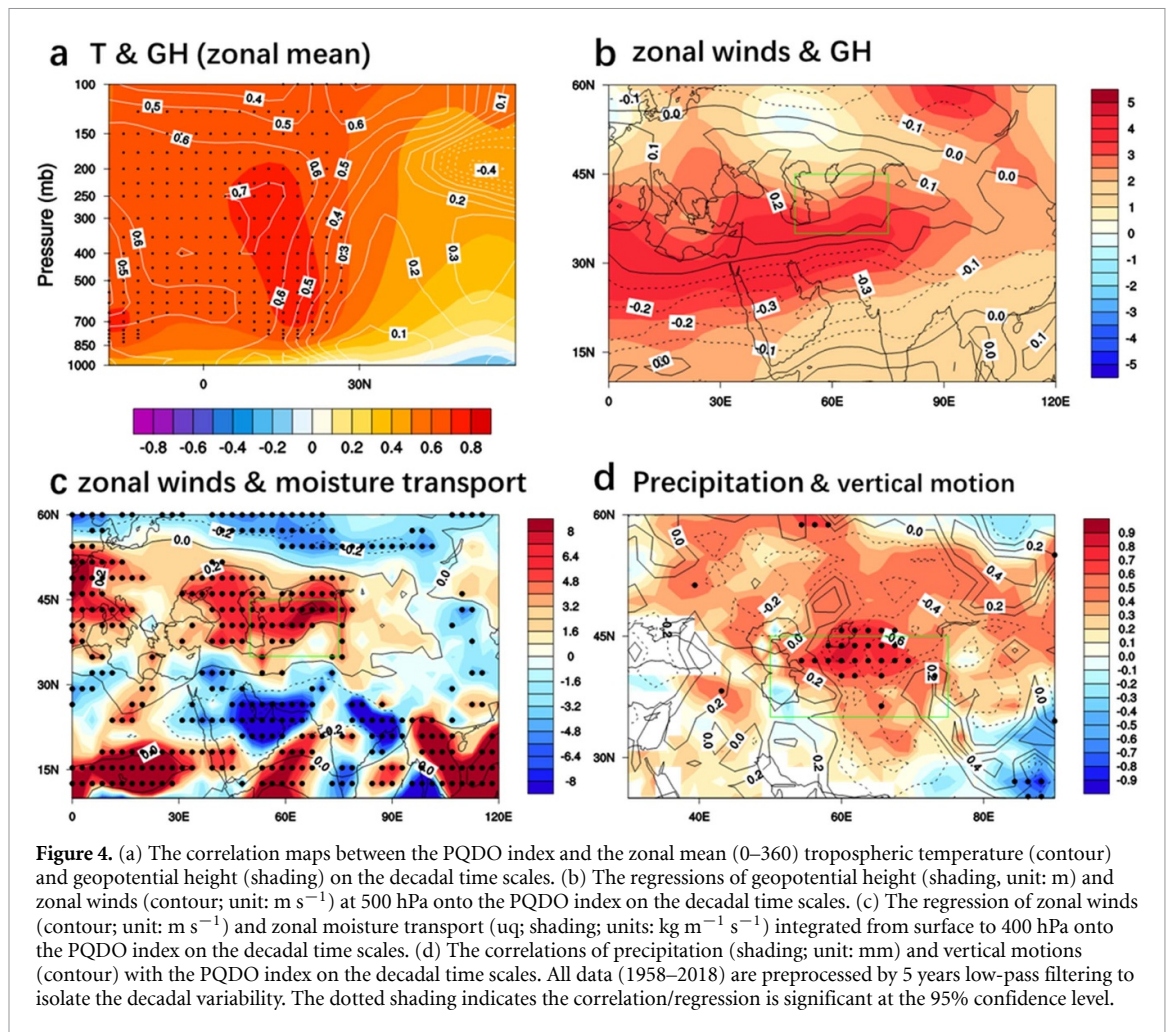
synchronized. Based on the above analysis, we can conclude that the decadal component of PQDO, Central Asian precipitation, and PDSI variabilities are highly coherent, with a synchronized 8–16 years period. In addition, an ensemble mean of the AMIP simulation (see section 2) indicates a consistently robust relationship between the PQDO and the Central Asian precipitation for the period 1979–2014, with a correlation coefficient reaching 0.61 on the inter-annual time scale (supplementary figure 2(a)). Note that there are biases between the simulated precipitation and PQDO after 2010. We further perform a 16 years (to cover the period of a cycle) running correlation between two series (supplementary figure 2(b)), which suggests that the coupled relationship between them is stable over time (running correlation coefficients >0.6 , significant at the 95% confidence level). Based on the above analysis, we hypothesize that the periodic decadal swings in the Central Asian dry/wet conditions are linked to the PQDO via the modulations of large-scale circulation and regional precipitation.

3.3. Mechanism

We first inspect how the PQDO influences the atmospheric circulations in CA on the decadal time scale (processed by the 5 years low-pass filtering). The correlations of air temperature and geopotential height with the PQDO are shown in figure 4(a). From a zonally-averaged perspective, due to the PQDO-related central Pacific SST warming, the entire troposphere is significantly heated in the tropical region. The upper-level shows more pronounced warming responses than the lower-level troposphere, and the warmed air is slightly asymmetrical to the equator, with a warm core located in the Northern Hemisphere. In contrast, the upper-level troposphere (especially at 200 hPa) displays significant cooling in the mid-high latitudes. As a result, the meridional temperature gradients over the Northern Hemisphere subtropics increase due to the ECP warming. Such a meridional contrast in air temperature would have a profound influence on atmospheric circulation. In figure 4(a), the geopotential height increases extensively in the tropical troposphere corresponded with warmer air, while the geopotential height responses over the mid-high latitudes are rather weak and insignificant, referring to an enlarged meridional contrast. We may also notice that the atmospheric responses to the tropical central Pacific heating are quasi-barotropic, with uniformly increased/decreased air temperature and geopotential in the entire troposphere. The impacts of PQDO are not limited to the central Pacific Ocean. More importantly, the PQDO-induced meridional contrasts would lead to the consequent geostrophic adjustments in zonal atmospheric circulations.

In addition to the zonal mean perspective, the responses of atmospheric circulation in CA to the PQDO are also examined. As shown in figure 4(b), the regression map of 500 hPa geopotential height onto the PQDO index indicate a strengthening Subtropical High on land. The anomalous geopotential height extends along the 30° N latitude, stretching from North Africa and the Mediterranean Sea to the western boundary of the Tibetan-Iran Plateau. In CA, the geopotential height decreases from south to north, exhibiting increased meridional gradients, which are consistent with the zonal mean results. Along both sides of the enhanced Subtropical High, strong wind anomalies are generated, with the westerlies strengthened in CA and easterlies prevailing in Iran Plateau and Arabian Peninsula. It must be noted that the PQDO-induced meridional geopotential height gradients significantly intensify the subtropical westerly jet, which is vital to the water vapor content and precipitation in CA [49]. As suggested in previous studies, the North Atlantic Ocean, Mediterranean Sea, Black Sea, and the Caspian Sea are important moisture sources for CA precipitation [50, 51]. By regressing the zonal moisture transport ($u \cdot q$ integrated from surface to 400 hPa) onto the PQDO index, strong zonal moisture transports are found along the enhanced subtropical westerly jet as is shown in figure 4(c). The strongest moisture convergence is located in CA, combining the water vapor transported from the Black Sea and the Caspian Sea. The PQDO-related strengthens in subtropical jet significantly increase the Central Asian water vapor supply by enhancing the moisture transport from the far west, which favors the regional precipitation.

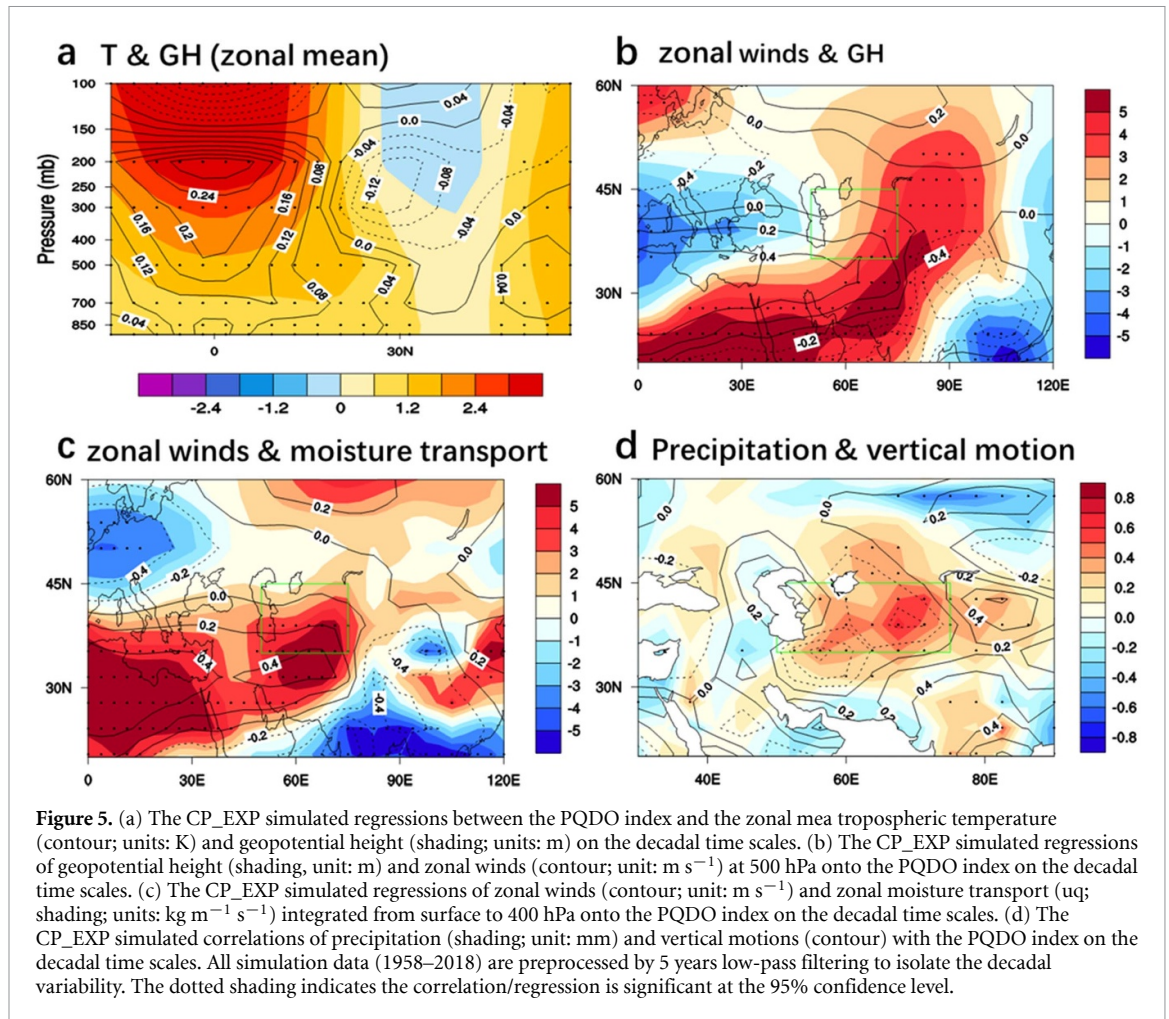
Figure 4(d) maps out the precipitation responses to the PQDO, which exhibits significantly increased rainfall in CA and shows noticeable consistency with the PQDO-related moisture transport. The central Pacific SST warming (PQDO) increases the meridional gradients of tropospheric temperature and geopotential height. It intensifies the water vapor transport by the subtropical westerlies, consequently resulting in more precipitation in CA. The coherence between the zonal winds and regional precipitation in CA highlights an important role of the eastward moisture transport in modulating the precipitation in association with the remote PQDO forcing. We may also notice that strong vertical motions are located on the east edge of CA, which somewhat correspond with the increased rainfall. The anomalous ascendant provides favorable dynamical conditions, which is as important as the zonal moisture transport to the regional precipitation. Thus, we may conclude that decadal swings observed in the Central Asian precipitation are mainly dominated by the increased moisture transport in response to the PQDO on the decadal time scale.



In the CP_EXP, the influences of PQDO on the atmospheric circulation and Central Asian precipitation are inspected. In figure 5(a), the regression map of the tropospheric temperature onto the PQDO displays prominent warming in the tropics but cooling in the subtropics, resulting in the enlarged meridional temperature gradients. The most significant temperature contrasts in response to the central Pacific heating are located at 200 hPa in the subtropical region. In association with the tropospheric warming, the geopotential height displays similar responses to the PQDO, exhibiting increased heights in the upper-level tropics. The simulated responses of temperature and geopotential height are overall consistent with the observed patterns, indicating that the PQDO-related central Pacific warming indeed enhances the meridional gradients in the Northern Hemisphere subtropics, which regulates the zonal circulation. As shown in figure 5(b), in response to the PQDO, the increased geopotential height extends from North Africa to central Siberia, while an anomalous low is located in the Mediterranean Sea, resulting in a significant incline of geopotential height in CA. The increased subtropical pressure gradients are consistent in both observation and CP_EXP simulation. Consequently, the subtropical westerly jet is

significantly strengthened in CA, transporting moisture from the North Atlantic Ocean and the Mediterranean Sea (figure 5(c)). Note that the westerly jet and the corresponding zonal moisture transport show southward shifts, which may be related to the inherent model biases. It has been suggested in the previous study [52] that the southward shift of the summer mean state of the westerly jet simulated by the ICTPAGCM may reflect the biases in reproducing the meridional temperature gradients. Such biases may be related to a lack of diurnal cycle in the model, which makes it difficult to the accurate representation of convection and sub-grid-scale vertical heat transport over the continents during the summer. Despite that the locations of the westerly jet show biases, the role of PQDO in strengthening the moisture transport in CA is successfully reproduced, which is consistent with the observation to some extent.

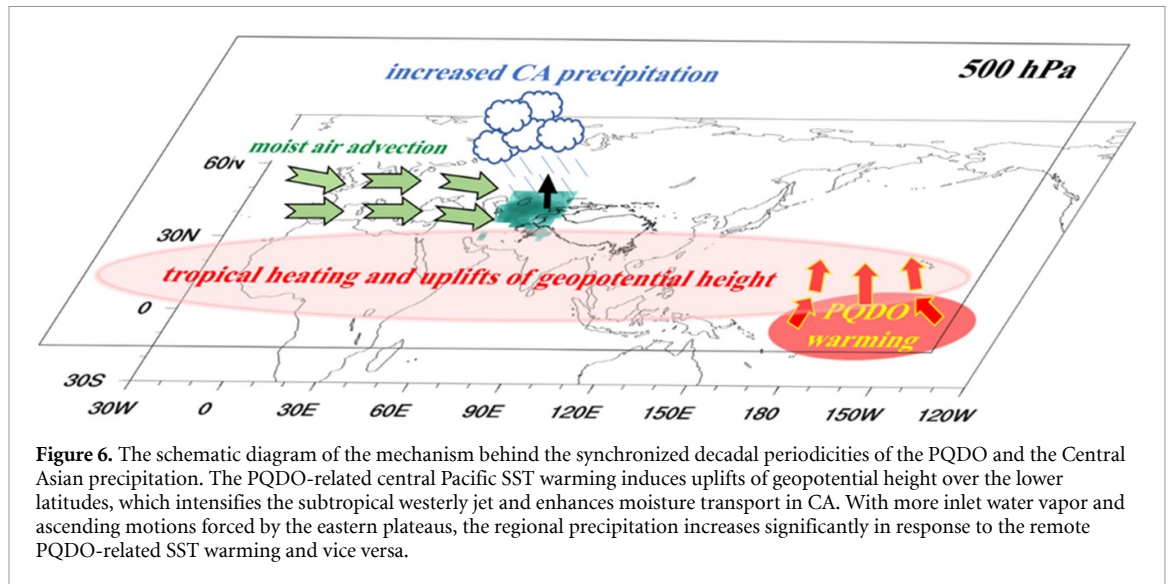
In figure 5(d), the intensified moisture transport and strongly increased precipitation are well corresponded, consistent with the observation. The model simulation indicates overall consistent results that the PQDO-related zonal moisture transport dominates the Central Asian precipitation on the decadal scale. Considering the coarse resolution of the ICTPAGCM, we also examine the results from the AMIP ensemble



(supplementary figure 3). The AMIP-simulated precipitation over the mid-latitudes shows a consistent increase in response to the PQDO on the decadal time scale. There is a significant positive correlation in CA, suggesting that the central Pacific SST warming corresponds well with the local increased rainfall. This is consistent with the results from the observation and the CP_EXP. In addition, the intensified westerlies are simulated by the AMIP ensemble, indicating an important role of the PQDO-induced zonal moisture transport in modulating the wet/dry conditions in CA.

It must be noted that strong vertical motions are consistently found in the observation and CP_EXP. In figure 5(d), the simulated profiles of ascendants are more confined to the 2000 m isoline on the east edge of CA, implying that the eastern terrains may play a role. CA is semi-surrounded by mountains and plateaus, such as the Tian Shan and Pamirs Plateau in the east, and Tibetan-Iran Plateau in the south/southeast, whereas CA is mainly flatland, and its elevation inclines to the east. It has been suggested in previous studies that the topography in CA enhances the responses of precipitation to remote climate modes (e.g. ENSO) [28, 53]. To discuss the effect of topography on the PQDO-related

Central Asian precipitation, we conducted an additional experiment with the East Asian topography removed (CP_EXP_NT). As shown in supplementary figure 4, the PQDO-induced meridional differences in geopotential height and temperature have little change, but the westerly jet and vertical motions are significantly weakened in CA. The moisture transport is no longer strong and withdraws to the Middle East. It indicates that the large terrains are not only important for the moisture convergence/ascendant in the foothill regions but also vital to the westward extension of the subtropical jet due to the surface heating and pumping effects in plateaus during the summer [54]. This is consistent with the previous studies that the Tibetan Plateau profoundly influences the atmospheric circulation in CA, such as the subtropical westerly jet and low-level cyclones [55, 56]. In addition to the direct meridional responses of atmospheric circulation and the predominate zonal moisture transport to the PQDO, the Central Asian topography may amplify in the PQDO-CA dry/wet conditions teleconnection by strengthening the regional scale vertical motion and the eastward moisture transport. The detailed impacts of topography on the Central Asian precipitation in addition to the PQDO-related moisture transport, are beyond



the scope of the current study and could be inspected in future works.

4. Discussion and conclusion

In this study, we identify periodic variability in the hydro-climatic system over CA. We find a decadal oscillation in CA dry/wet conditions consistently indicated by the PDSI and soil moisture, with a significant period of 8–16 years. Further analysis suggests that the periodicity of dry/wet conditions arises from the oscillatory variations in regional precipitation, whereas the temperature only exhibits a long-term warming trend. Observational analysis suggests that the PQDO is very likely a dominating driver of the periodic decadal swings observed in the Central Asian precipitation and, consequently, the regional dry/wet conditions. The schematic diagram is provided in figure 6. The PQDO-related ECP warming induces the zonally distributed tropospheric warming in the tropics, which corresponds with the increased meridional contrasts in the subtropical regions. The subtropical westerly jet is strengthened in CA, further enhancing the zonal moisture transport from the North Atlantic Ocean and the Mediterranean Sea and resulting in more precipitation in the heart of CA. Moreover, the large-scale orography east of CA may play a role by enhancing the eastward extension of the anomalous westerly responses due to the heat pumping effects over the plateaus. Also, significant moisture convergence and ascending motions in the foothill regions may amplify the precipitation in response to the PQDO. The CP_EXP successfully reproduces the above mechanism, and the results are overall consistent, indicating a robust synchronization of Central Asian dry/wet conditions to the PQDO.

We may notice that the eastern Indian Ocean is also correlated with the Central Asian precipitation.

The quasi-decadal variabilities of SST in the ECP Ocean and the eastern Indian Ocean are overall synchronized [57], which may result in a consistent SST warming signal in the Indian Ocean. However, a previous study also indicated that, on the interannual scale, while the ENSO-related central-eastern Pacific SST warming favors the regional precipitation, the effects of Indian Ocean SST are the opposite [58]. The relative contributions of the Indian Ocean SST on the Central Asian precipitation in addition to the PQDO may be comprehensively assessed in future works.

The decadal swings of dry/wet conditions in CA and its coupled relationship with the PQDO can be reproduced by most of the state-of-the-art models in AMIP simulations. The SST-precipitation relationship could be further evaluated with more available model simulation results. We also construct a PQDO-based linear regression model using observations (supplementary figure 5), which also captures the decadal swings of precipitation. SST is more predictable than inland precipitation [59]. Thus, based on the linear regression model, the Central Asian precipitation can be better constrained using the model-predicted SST in the central Pacific. According to previous studies [12], the decadal periodicity of the PQDO is physically-based. The PQDO is currently in the transition phase of the cycle, from the positive phase to the negative, which may indicate that CA is about to get dryer in the next decade. Therefore, based on this newly discovered oscillatory feature, we may significantly improve the predictability of CA dry/wet conditions several years in advance.

Data availability statement

All data that support the findings of this study are included within the article (and any supplementary files).

Acknowledgments

This work is jointly supported by the National Key Research and Development Program of China (2020YFA0608401), National Natural Science Foundation of China (41975082), and National Programme on Global Change and Air-Sea Interaction (GASI-IPOVAI-06 and GASI-IPOVAI-03).

Conflict of interest

Authors declare that they have no competing interests.

ORCID iDs

Cheng Sun  <https://orcid.org/0000-0003-0474-7593>

Zengchao Hao  <https://orcid.org/0000-0001-7666-7053>

References

- [1] Ghil M 2002 Natural climate variability *Encyclopedia of Global Environmental Change* vol 1 pp 544–9
- [2] Baldwin M et al 2001 The quasi-biennial oscillation *Rev. Geophys.* **39** 179–229
- [3] Lindzen R S and Holton J R 1968 A theory of the quasi-biennial oscillation *J. Atmos. Sci.* **25** 1095–107
- [4] Rasmusson E M, Wang X and Ropelewski C F 1990 The biennial component of ENSO variability *J. Mar. Syst.* **1** 71–96
- [5] Rasmusson E M and Carpenter T H 1982 Variations in tropical sea surface temperature and surface wind fields associated with the southern oscillation/El Niño *Mon. Weather Rev.* **110** 354–84
- [6] Emanuel K 2005 Increasing destructiveness of tropical cyclones over the past 30 years *Nature* **436** 686–8
- [7] Swanson K L, Sugihara G and Tsonis A A 2009 Long-term natural variability and 20th century climate change *Proc. Natl Acad. Sci.* **106** 16120–3
- [8] Barnston A G and Livezey R E 1987 Classification, seasonality and persistence of low-frequency atmospheric circulation patterns *Mon. Weather Rev.* **115** 1083–126
- [9] Wallace J M and Gutzler D S 1981 Teleconnections in the geopotential height field during the northern hemisphere winter *Mon. Weather Rev.* **109** 784–812
- [10] Allan R J 2000 ENSO and climatic variability in the last 150 years. El Niño and the Southern Oscillation: multiscale variability, global and regional impacts
- [11] Tourre Y M, Rajagopalan B, Kushnir Y, Barlow M and White W B 2001 Patterns of coherent decadal and interdecadal climate signals in the Pacific basin during the 20th century *Geophys. Res. Lett.* **28** 2069–72
- [12] Jin C, Bin W and Jian L 2021 Emerging Pacific quasi-decadal oscillation over the past 70 years *Geophys. Res. Lett.* **48** e2020GL090851
- [13] White W B, Dettinger M D and Cayan D R 2003 Sources of global warming of the upper ocean on decadal period scales *J. Geophys. Res. Oceans* **108** 3248
- [14] White W B and Liu Z 2008 Resonant excitation of the quasi-decadal oscillation by the 11-year signal in the sun's irradiance *J. Geophys. Res. Oceans* **113** C01002
- [15] White W B, Tourre Y M, Barlow M and Dettinger M 2003 A delayed action oscillator shared by biennial, interannual, and decadal signals in the Pacific Basin *J. Geophys. Res. Oceans* **108** 3070
- [16] Wang S, Hakala K, Gillies R R and Capehart W J 2014 The Pacific quasi-decadal oscillation (QDO): an important precursor toward anticipating major flood events in the Missouri River Basin? *Geophys. Res. Lett.* **41** 991–7
- [17] Wang S-Y, Gillies R R, Hipps L E and Jin J 2011 A transition-phase teleconnection of the Pacific quasi-decadal oscillation *Clim. Dyn.* **36** 681–93
- [18] Wang S-Y, Gillies R R, Jin J and Hipps L E 2010 Coherence between the great salt lake level and the Pacific quasi-decadal oscillation *J. Clim.* **23** 2161–77
- [19] Wang S-Y and Gillies R R 2013 Influence of the Pacific quasi-decadal oscillation on the monsoon precipitation in Nepal *Clim. Dyn.* **40** 95–107
- [20] Huang W-R, Wang S-Y S and Guan B T 2018 Decadal fluctuations in the western Pacific recorded by long precipitation records in Taiwan *Clim. Dyn.* **50** 1597–608
- [21] Cowan P J 2007 Geographic usage of the terms middle Asia and Central Asia *J. Arid Environ.* **69** 359–63
- [22] Qi J, Bobushev T S, Kulmatov R, Groisman P and Gutman G 2012 Addressing global change challenges for Central Asian socio-ecosystems *Front. Earth Sci.* **6** 115–21
- [23] Hu Z, Zhang C, Hu Q and Tian H 2014 Temperature changes in Central Asia from 1979 to 2011 based on multiple datasets *J. Clim.* **27** 1143–67
- [24] Guo H, Chen S, Bao A, Hu J, Gebregiorgis A, Xue X and Zhang X 2015 Inter-comparison of high-resolution satellite precipitation products over Central Asia *Remote Sens.* **7** 7181–211
- [25] Dai A 2013 Increasing drought under global warming in observations and models *Nat. Clim. Change* **3** 52–58
- [26] Lioubimtseva E and Henebry G M 2009 Climate and environmental change in arid Central Asia: impacts, vulnerability, and adaptations *J. Arid Environ.* **73** 963–77
- [27] Hu Z, Hu Q, Zhang C, Chen X and Li Q 2016 Evaluation of reanalysis, spatially interpolated and satellite remotely sensed precipitation data sets in Central Asia *J. Geophys. Res. Atmos.* **121** 5648–63
- [28] Chen Z, Wu R, Zhao Y and Wang Z 2021 Different responses of Central Asian precipitation to strong and weak El Niño events *J. Clim.* **35** 1497–514
- [29] de Beurs K M, Henebry G M, Owsley B C and Sokolik I N 2018 Large scale climate oscillation impacts on temperature, precipitation and land surface phenology in Central Asia *Environ. Res. Lett.* **13** 065018
- [30] Bothe O, Fraedrich K and Zhu X 2012 Precipitation climate of Central Asia and the large-scale atmospheric circulation *Theor. Appl. Climatol.* **108** 345–54
- [31] Hu Z, Zhou Q, Chen X, Qian C, Wang S and Li J 2017 Variations and changes of annual precipitation in Central Asia over the last century *Int. J. Climatol.* **37** 157–70
- [32] Zhong L, Hua L, Yao Y and Feng J 2021 Interdecadal aridity variations in Central Asia during 1950–2016 regulated by oceanic conditions under the background of global warming *Clim. Dyn.* **56** 3665–86
- [33] Guo H, Bao A, Liu T, Jiapaer G, Ndayisaba F, Jiang L, Kurban A and de Maeyer P 2018 Spatial and temporal characteristics of droughts in Central Asia during 1966–2015 *Sci. Total Environ.* **624** 1523–38
- [34] Hu Z, Chen X, Chen D, Li J, Wang S, Zhou Q, Yin G and Guo M 2019 'Dry gets drier, wet gets wetter': a case study over the arid regions of Central Asia *Int. J. Climatol.* **39** 1072–91
- [35] Abatzoglou J T, Dobrowski S Z, Parks S A and Hegewisch K C 2018 Terraclimate, a high-resolution global dataset of monthly climate and climatic water balance from 1958–2015 *Sci. Data* **5** 1–12
- [36] van der Schrier G, Barichivich J, Briffa K and Jones P D 2013 A scPDSI-based global data set of dry and wet spells for 1901–2009 *J. Geophys. Res. Atmos.* **118** 4025–48
- [37] Huang B, Thorne P W, Banzon V F, Boyer T, Chepurin G, Lawrimore J H, Menne M J, Smith T M, Vose R S and Zhang H-M 2017 Extended reconstructed sea surface temperature, version 5 (ERSSTv5): upgrades, validations, and intercomparisons *J. Clim.* **30** 8179–205

- [38] Kobayashi S *et al* 2015 The JRA-55 reanalysis: general specifications and basic characteristics *J. Meteorol. Soc. Japan Ser. II* **93** 5–48
- [39] Gates W L *et al* 1999 An overview of the results of the Atmospheric Model Intercomparison Project (AMIP i) *Bull. Am. Meteorol. Soc.* **80** 29–56
- [40] Heim R R Jr 2002 A review of twentieth-century drought indices used in the United States *Bull. Am. Meteorol. Soc.* **83** 1149–66
- [41] Vicente-Serrano S M, Beguería S and López-Moreno J I 2010 A multiscalar drought index sensitive to global warming: the standardized precipitation evapotranspiration index *J. Clim.* **23** 1696–718
- [42] Palmer W C 1965 *Meteorological Drought* (Washington, DC: US Department of Commerce, Weather Bureau)
- [43] Guttman N B 1998 Comparing the palmer drought index and the standardized precipitation index 1 *JAWRA J. Am. Water Resour. Assoc.* **34** 113–21
- [44] Torrence C and Compo G P 1998 A practical guide to wavelet analysis *Bull. Am. Meteorol. Soc.* **79** 61–78
- [45] Kucharski F, Parvin A, Rodriguez-Fonseca B, Farneti R, Martin-Rey M, Polo I, Mohino E, Losada T and Mechoso C R 2016 The teleconnection of the tropical Atlantic to Indo-Pacific sea surface temperatures on inter-annual to centennial time scales: a review of recent findings *Atmosphere* **7** 29
- [46] Grinsted A, Moore J C and Jevrejeva S 2004 Application of the cross wavelet transform and wavelet coherence to geophysical time series *Nonlinear Process. Geophys.* **11** 561–6
- [47] Sun C, Li J and Jin F-F 2015 A delayed oscillator model for the quasi-periodic multidecadal variability of the NAO *Clim. Dyn.* **45** 2083–99
- [48] Peng D, Zhou T, Zhang L and Zou L 2019 Detecting human influence on the temperature changes in Central Asia *Clim. Dyn.* **53** 4553–68
- [49] Peng D, Zhou T and Zhang L 2020 Moisture sources associated with precipitation during dry and wet seasons over Central Asia *J. Clim.* **33** 10755–71
- [50] Guan X, Yang L, Zhang Y and Li J 2019 Spatial distribution, temporal variation, and transport characteristics of atmospheric water vapor over Central Asia and the arid region of china *Glob. Planet. Change* **172** 159–78
- [51] Yin Z-Y, Wang H and Liu X 2014 A comparative study on precipitation climatology and interannual variability in the lower midlatitude East Asia and Central Asia *J. Clim.* **27** 7830–48
- [52] Molteni F 2003 Atmospheric simulations using a GCM with simplified physical parametrizations. I: model climatology and variability in multi-decadal experiments *Clim. Dyn.* **20** 175–91
- [53] Abid M A, Almazroui M, Kucharski F, O'Brien E and Yousef A E 2018 Enso relationship to summer rainfall variability and its potential predictability over Arabian Peninsula region *npj Clim. Atmos. Sci.* **1** 1–7
- [54] Wu G, Liu Y, Zhang Q, Duan A, Wang T, Wan R, Liu X, Li W, Wang Z and Liang X 2007 The influence of mechanical and thermal forcing by the Tibetan Plateau on Asian climate *J. Hydrometeorol.* **8** 770–89
- [55] Babaei M, Alizadeh O and Irannejad P 2021 Impacts of orography on large-scale atmospheric circulation: application of a regional climate model *Clim. Dyn.* **57** 1973–92
- [56] White R, Battisti D and Roe G 2017 Mongolian mountains matter most: impacts of the latitude and height of Asian orography on pacific wintertime atmospheric circulation *J. Clim.* **30** 4065–82
- [57] Allan R, Reason C, Lindesay J and Ansell T J 2003 Protracted ENSO episodes and their impacts in the Indian Ocean region *Deep Sea Res. Part II Top. Stud. Oceanogr.* **50** 2331–47
- [58] Mariotti A 2007 How ENSO impacts precipitation in southwest Central Asia *Geophys. Res. Lett.* **34** L16706
- [59] Wang B *et al* 2009 Advance and prospectus of seasonal prediction: assessment of the APCC/CliPAS 14-model ensemble retrospective seasonal prediction (1980–2004) *Clim. Dyn.* **33** 93–117